Optical properties and molecular compositions of water-soluble and water-insoluble brown carbon (BrC) aerosols in Northwest China

Jianjun Li[1,2], Qi Zhang[2,*], Gehui Wang[1,3,4,*], Jin Li[1], Can Wu[1,3], Lang Liu[1], Jiayuan Wang[1,2], Wenqing Jiang[2], Lijuan Li[1,2], Kin Fai Ho[1,5], Junji Cao[1]

[1] Key Lab of Aerosol Chemistry & Physics, SKLLQG, Institute of Earth Environment, Chinese Academy of Sciences, Xi'an 710061, China
[2] Department of Environmental Toxicology, University of California, Davis, CA 95616, USA
[3] Key Laboratory of Geographic Information Science of the Ministry of Education, School of Geographic Sciences, East China Normal University, Shanghai 200241, China
[4] Institute of Eco-Chongming, 3663 N. Zhongshan Rd., Shanghai 200062, China
[5] The Jockey Club School of Public Health and Primary Care, The Chinese University of Hong Kong, Hong Kong, China

*Corresponding authors:
Prof. Qi Zhang
Department of Environmental Toxicology, University of California, Davis
One Shields Avenue, Davis, CA 95616
Phone: 1-530-752-5779
Fax: 1-530-752-3394
Email: dkwzhang@ucdavis.edu;

Prof. Gehui Wang
School of Geographic Sciences, East China Normal University, Shanghai, China
500 Dongchuan Rd., Shanghai 200241, China
Phone: 86-21-5434-1193
E-mail: ghwang@geo.ecnu.edu.cn.

Abstract

Brown carbon (BrC) contributes significantly to aerosol light absorption, thus can affect the earth's radiation balance and atmospheric photochemical processes. In this study, we examined the light absorption properties and molecular compositions of water-soluble (WS-BrC) and water-insoluble (WI-BrC) BrC in $PM_{2.5}$ collected from a rural site in the Guanzhong Basin – a highly polluted region in Northwest China. Both WS-BrC and WI-BrC showed elevated light absorption coefficients (Abs) in winter (4-7 times of those in summer) mainly attributed to enhanced emissions from residential biomass burning (BB) for house heating. While the average mass absorption coefficients at 365 nm (MAC_{365}) of WS-BrC were similar between daytime and nighttime in summer (0.99±0.17 and 1.01±0.18 $m^2\ g^{-1}$, respectively), the average MAC_{365} of WI-BrC was more than a factor of 2 higher during daytime (2.45±1.14 $m^2\ g^{-1}$) than at night (1.18±0.36 $m^2\ g^{-1}$). This difference was partly attributed to enhanced photochemical formation of WI-BrC species, such as oxygenated polycyclic aromatic hydrocarbons (OPAHs). In contrast, the MACs of WS-BrC and WI-BrC were generally similar in winter and both showed little diel differences. The Abs of wintertime WS-BrC correlated strongly with relative humidity, sulfate, and NO_2, suggesting that aqueous-phase reaction is an important pathway for secondary BrC formation during the winter season in Northwest China. Nitrophenols on average contributed 2.44±1.78% of the Abs of WS-BrC in winter, but only 0.12±0.03% in summer due to faster photodegradation reactions. WS-BrC and WI-BrC were estimated to account for 0.83±0.23% and 0.53±0.33%, respectively, of the total down-welling solar radiation in the UV range in summer, and 1.67±0.72% and 2.07±1.24%, respectively, in winter. The total absorption by BrC in the UV region was about 55-79% relative to the elemental carbon (EC) absorption.

53 Keywords: Brown Carbon (BrC); Organic Aerosol; Optical Property; Molecular Composition

54

1. Introduction

Light-absorbing organic matter, termed as “brown carbon (BrC)”, has been recognized as an important climate forcer due to its ability to directly interact with both incoming solar radiation and outgoing terrestrial radiation (Andreae and Gelencser, 2006;Laskin et al., 2015). BrC is a complex mixture of organic compounds, which collectively show a light absorption profile increasing exponentially from the visible (Vis) to the ultraviolet (UV) range. Due to the high abundance of organic aerosol in continental regions, especially in places with intensive anthropogenic pollution, the contribution of BrC to aerosol absorption in the near-UV range is potentially significant (Kirillova et al., 2014b;Huang et al., 2018;Yan et al., 2015a). For example, a model study showed that BrC contributes up to +0.25 W m^{-2} of radiative forcing on a planetary scale, which is approximately 19% of the absorption by anthropogenic aerosols (Feng et al., 2013). Moreover, the strong absorption of BrC in the UV spectral region can reduce the solar actinic flux, and subsequently affect atmospheric photochemistry and tropospheric ozone production (Jacobson, 1998;Mohr et al., 2013).

A thorough understanding of the sources and transformation processes of BrC in the atmosphere is important, but it is still lacking. Biomass/biofuel combustion, including forest fires, and burning of wood and agricultural wastes for residential cooking and heating, has been shown as a particularly important source of BrC (Washenfelder et al., 2015;Desyaterik et al., 2013;Lin et al., 2017). BrC can also be emitted directly from coal burning (Yan et al., 2017), and biogenic release of fungi, plant debris, and humic matter (Rizzo et al., 2013;Rizzo et al., 2011). In addition, recent studies suggested that secondary BrC can be formed through various reaction pathways, including photooxidation of aromatic volatile organic compounds (VOCs) (Lin et al., 2015;Liu et

al., 2016), reactive uptake of isoprene epoxydiols onto preexisting sulfate aerosols (Lin et al., 2014), aqueous oxidation of phenolic compounds and α-dicarbonyls (Chang and Thompson, 2010;Nozière and Esteve, 2005;Smith et al., 2016;Yu et al., 2014;Xu et al., 2018), and reactions of ammonia or amines with carbonyl compounds in particles or cloud droplets (Nozière et al., 2007;Laskin et al., 2010;Updyke et al., 2012;Nguyen et al., 2012;De Haan et al., 2018;Powelson et al., 2014). However, atmospheric oxidation processes may also cause "photobleach" – photodegradation of BrC into less light-absorbing compounds (Lee et al., 2014;Romonosky et al., 2015;Sumlin et al., 2017), which may complicate the understanding of BrC in the atmosphere.

A common way to quantify the absorption properties of BrC is to measure the absorbance of aerosol extracts over a wide wavelength range using spectrophotometers. This approach can differentiate the interference of black carbon (BC) or mineral dust (Hecobian et al., 2010). Most of the studies use ultrapure water to extract organic substance in the aerosol, and thus measure the optical properties of water-soluble BrC (WS-BrC) (Wu et al., 2019;Hecobian et al., 2010;Kirillova et al., 2014b). In addition, some studies analyzed the light absorption of BrC extracted using polar organic solvents such as methanol or acetone (Liu et al., 2013;Huang et al., 2018;Kim et al., 2016). Since such extracts contain both water-soluble and water-insoluble chromophores, little information is available regarding the contribution and formation of water-insoluble BrC (WI-BrC). However, it is important to understand WI-BrC given the facts that some water-insoluble organic compounds, such as polycyclic aromatic hydrocarbons and their derivatives, are effective light absorbers and that the mass absorption of WI-BrC could be even greater than that of the water-soluble fraction (Chen and Bond, 2010;Huang et al., 2018;Sengupta et al., 2018). Thus, it is necessary to extract water-soluble and water-insoluble organic components separately, e.g., via

using solvents with different polarity in sequence. Combining with measurements of BrC molecular compositions, the UV-vis absorption properties of the water-soluble and water-insoluble extracts may help us better understand the sources and formation mechanisms of light-absorbing compounds in the atmosphere.

China has been experiencing serious atmospheric pollution conditions in recent decades, and both model and field results showed elevated light absorption of BrC in most regions of China (Huang et al., 2018;Cheng et al., 2011;Yan et al., 2017;Li et al., 2016b) compared to developed countries such as the U.S. (Hecobian et al., 2010;Washenfelder et al., 2015) and European countries (Mohr et al., 2013;Teich et al., 2017). However, BrC-related data are scarce in the Guanzhong Basin (Shen et al., 2017;Huang et al., 2018), which is one of the most polluted regions in China (van Donkelaar et al., 2010). Here we present measurements of the optical properties of WS-BrC and WI-BrC in $PM_{2.5}$ collected from a rural area of the Guanzhong Basin during winter and summer seasons. We also measured the concentrations of several BrC compounds as well as those of organic carbon (OC), elemental carbon (EC), water-soluble OC (WSOC) and inorganic ions. These data were analyzed to examine the effects of sources emissions, daytime photochemical oxidation, and aqueous-phase chemistry on WS- and WI-BrC components in different seasons.

2. Experimental section

2.1 Sample collection

The sampling was conducted at a small village (namely Lincun, 34º44′ N and 109º32′E, 354m a.s.l.) ~ 40 km northeast to Xi'an, the capital of Shaanxi Province (Figure S1). The sampling site is located in the central part of Guanzhong Basin with no obvious point source of air pollutants in

the surrounding areas. $PM_{2.5}$ samples were collected twice a day (~8 am to 8 pm and ~8 pm to 8 am) onto prebaked (450 ^{o}C, 6-8 hr) quartz fiber filters (Whatman, QM-A, USA) during Aug. 3-23, 2016 and Jan. 20-Feb. 1, 2017 using a TISCH Environmental (USA) $PM_{2.5}$ high volume (1.13 m^3 min^{-1}) sampler. Field blank samples were also collected by mounting blank filters onto the sampler for about 15 min without pumping any air. After sampling, the sample filters were immediately sealed in aluminum foil bags, and then stored in a freezer (−5 ^{o}C) prior to analysis. Meteorological conditions, and concentrations of O_3 and NO_2 during this studied period are presented in Figure 1.

2.2 Filter extraction and absorption spectra analysis

For each $PM_{2.5}$ sample, a portion of the filter (~13.384 cm^2) was first extracted in 8 ml of Milli-Q water (18.2 MΩ) through 30 min of sonication at ~ 0^{o}C. The water extract was then filtered via vacuum filtration with a 25mm diameter 5 μm pore hydrophobic PTFE membrane filter (Merck Millipore Ltd, Mitex^{TM} Membrane Filters, USA). Afterwards, the insoluble PM components collected on the PTFE membrane filter and remained on the sample filter were rinsed with 2 ml Milli-Q water, air dried, and then extracted via sonication in 8 ml pure acetonitrile (ACN) (Honeywell Burdick & Jackson, LC/MS Grade, USA). The acetonitrile extract was filtered via a 13 mm diameter 0.45 μm pore syringe filter (PALL, Bulk Acrodisc®, PTFE Membrane Filters, USA). The light absorption spectra of the water and the acetonitrile extracts were measured between 190 nm to 820 nm by a diode-array spectrophotometer (Hewlett Packard 8452A, USA) using quartz cuvettes with 1 cm length path. Field blank filters were extracted and measured in the same manner as the samples. Data presented in this study were corrected for the field blanks (<10% relative to field samples).

2.3 Chemical Analysis

OC and EC were analyzed using DRI Carbon Analyzer (Model 2001, USA). Another piece of the filter sample (~8.6 cm^2) was extracted with Milli-Q water (18.2MΩ), and filtered through a PTFE syringe filter. Then the water-extract was analyzed for water-soluble inorganic ions (SO_4^{2-}, NO_3^-, NH_4^+, Cl^-, F^-, Ca^{2+}, K^+, Na^+ and Mg^{2+}) using a Metrohm Ion Chromatography (Metrohm 940, Switzerland) and WSOC using a Shimadzu TOC analyzer (TOC-L CPH, Japan) and. Concentrations of individual molecules, including levoglucosan, parent-PAHs, Oxygenated-PAHs (OPAHs), nitrophenols, isoprene and α-/β-pinene derived products, were measured using GC/EI-MS (Agilent 7890A-5975C, USA) calibrated by authentic standards. More details on these measurements can be found in previous publications (Li et al., 2014).

2.4 Data Interpretation

In this study, water-insoluble OC (WIOC) was calculated by the difference between OC and WSOC:

$$M_{WIOC} = M_{OC} - M_{WSOC} \qquad (1)$$

where M_{WIOC}, M_{OC}, and M_{WSOC} correspond to the mass concentration (in μgC m^{-3}) of WIOC, OC, and WSOC, respectively, in the air.

The absorption coefficient of WS-BrC ($Abs_{\lambda,WS\text{-}BrC}$, Mm^{-1}) or WI-BrC ($Abs_{\lambda,WI\text{-}BrC}$, Mm^{-1}) at a given wavelength (λ) is determined from the UV-vis spectrum of the water extract (Hecobian et al., 2010;Laskin et al., 2015)

$$Abs_\lambda = (A_\lambda - A_{700}) \times \frac{V_{solvent}}{V_a \times l} \times \ln(10) \times 100 \qquad (2)$$

where A_λ is the absorbance of the water ($A_{\lambda,WS\text{-}BrC}$) or ACN ($A_{\lambda,WI\text{-}BrC}$) extract at λ, which is corrected for the field blank. $V_{solvent}$ (ml) is the volume of solvent (water or ACN) used to extract the filter (8 mL), and Va (m^3) is the air volume passed through the filter punch. *l* (cm) is the

optical length of the quartz cuvettes used for UV-vis measurement and ln(10) is used to convert the logbase-10 (provided by the spectrophotometer) to natural logarithm. 100 is for unit conversion. A_{700} (absorbance at the wavelength of 700 nm) is subtracted to minimize the interference of baseline shift. The mass absorption coefficient of WS-BrC ($MAC_{\lambda,WS\text{-}BrC}$, $m^2\ g^{-1}$) or WI-BrC ($MAC_{\lambda,WI\text{-}BrC}$, $m^2\ g^{-1}$) at wavelength of λ is calculated using eq (3)

$$MAC_{\lambda} = \frac{Abs_{\lambda}}{M} \qquad (3)$$

where M is the mass concentration of WSOC or WIOC. Note that since it is possible that not all the WI-BrC was extracted into ACN, the $Abs_{\lambda,WI\text{-}BrC}$ (estimated uncertainty is 32%) and $MAC_{\lambda,WI\text{-}BrC}$ (estimated uncertainty is 33%) reported in this study are likely the lower bound values. Nevertheless, the underestimation is probably insignificant since Chen and Bond (Chen and Bond, 2010) reported that >92% of BrC was extractable by organic solvents (methanol or acetone).

The wavelength dependence for BrC absorption is fit with a power law equation:

$$Abs_{\lambda} = K \times \lambda^{-AAE} \qquad (4)$$

where K is a constant and AAE stands for absorption Ångström exponent. In this study, the AAE for a given sample is calculated through the linear regression of $\log(Abs_{\lambda})$ against $\log \lambda$ between 300−450 nm. This wavelength range is chosen because the fits of all the samples in this study are better than r^2=0.99. Note that slightly higher AAE values (by up to 10%) are obtained using a wider wavelength range (e.g., 300-550 nm; Figure S2).

The fraction of solar irradiance absorbed by particulate BrC at a given wavelength λ is estimated following the Beer−Lambert's law:

$$\frac{I_0 - I}{I_0}(\lambda) = 1 - e^{-b_{ap,\lambda,x} \times h_{ABL}} \qquad (5)$$

where *x* denotes WS-BrC or WI-BrC, h_{ABL} is the atmospheric boundary layer height (assuming 1200 m in summer and 600 m in winter) according to the assumption that the ground measurement results are representative of the average values in the whole planetary boundary layer (PBL) (Kirchstetter et al., 2004;Kirillova et al., 2014a). I_0 denotes the incident solar radiance in the form of either actinic flux (in quanta s^{-1} cm^{-2} nm^{-1}) or irradiance (in W m^{-2} nm^{-1}), which were obtained using the TUV Quick Calculator (http://cprm.acom.ucar.edu/Models/TUV/Interactive_TUV/). (I_0-I) denotes the direct absorption of solar actinic flux or irradiance by BrC. $b_{ap,\lambda,x}$ corresponds to the absorption coefficient ($b_{ap,}$ m^{-1}) of WS-BrC or WI-BrC at wavelength of λ. The absorption properties of BrC extracted by bulk solution may not entirely reflect the light absorption by ambient aerosols. However, an estimated conversion factor can be calculated from the light absorption of size-resolved samples using the Mie theory. Assuming that particles are of spherical morphology and externally mixed with other light-absorbing components, an imaginary refractive index (*k*, responsible for absorption) could be obtained from MAC using follow equation (Laskin et al., 2015):

$$k_{(\lambda)} = \frac{\rho \times \lambda \times Abs_{\lambda}}{4\pi \times M_{WSOC}} = \frac{\rho \times \lambda \times MAC_{\lambda}}{4\pi} \quad (6)$$

where ρ (g/cm3) was particle density and assigned as 1.5, and more details about Mie theory calculations can be referred to the study by Liu et al. (2013). Previous studies showed that the light absorption coefficient of particulate BrC ($b_{ap,\lambda,BrC}$) is around 0.7−2.0 times of that from bulk solution ($Abs_{\lambda,WS\text{-}BrC\ or\ WI\text{-}BrC}$) (Liu et al., 2013;Sun et al., 2007). Here, a conversion factor of 1.3 is applied based on a Mie theory calculation of aerosols in Xi'an (~ 40 km away from the sampling site) (Wu, 2018).

3. Results and Discussion

3.1 Optical absorption characteristics of WS-BrC and WI-BrC

The average absorption spectra of WS-BrC and WI-BrC (λ = 300-700 nm) during daytime and nighttime in different seasons are shown in Figure 2a &b. The absorption Ångström exponents for both WS-BrC ($AAE_{WS\text{-}BrC}$) and WI-BrC ($AAE_{WI\text{-}BrC}$) are generally higher than 5, verifying the contribution of BrC to aerosol absorptivity in the region. The average $AAE_{WS\text{-}BrC}$ are similar between summer (5.43±0.41) and winter (5.11±0.53). Huang et al. (2014) and Shen et al. (2017) reported comparable $AAE_{WS\text{-}BrC}$ values (5.3-5.7) with no significant seasonal change at urban sites of Xi'an, suggesting common characteristics of BrC on a regional scale in the Guanzhong Basin of China. These results are comparable with the data reported in Guangzhou (5.3) (Liu et al., 2018), but much lower than those in Beijing (5.3-7.3) (Cheng et al., 2011;Yan et al., 2015b;Du et al., 2014) and Nanjing (6.7-7.3) (Chen et al., 2018). Moreover, comparable AAE values were reported for WS-BrC in Switzerland (3.8-5.1) (Moschos et al., 2018) and Nepal (4.2-5.6) (Wu et al., 2019;Kirillova et al., 2016), but higher $AAE_{WS\text{-}BrC}$ were found in southeastern US (7 ± 1) (Hecobian et al., 2010), Los Angeles Basin (7.6 ± 0.5) (Zhang et al., 2013), and Korea (5.84-9.17) (Kim et al., 2016).

The $AAE_{WI\text{-}BrC}$ shows more obvious seasonal variations with a higher average value in winter (6.04±0.22) than in summer (5.01±0.58). This difference suggests that the chemical composition of WI-BrC might be more different in different seasons, due to variations in the sources and atmospheric formation and aging processes of light absorbing hydrophobic compounds.

The light absorption properties of WS-BrC and WI-BrC present obvious seasonal variations (Figure 2). The average (±1σ) Abs and MAC values of BrC at 365 nm (i.e., $Abs_{365,WS\text{-}BrC}$,

231 $Abs_{365,WI\text{-}BrC}$, $MAC_{365,WS\text{-}BrC}$, and $MAC_{365,WI\text{-}BrC}$) during daytime and nighttime in winter and
232 summer are summarized in Table 1. 365 nm was chosen to avoid interferences from inorganic
233 compounds (e.g., nitrate and nitrite) and to be consistent with previous studies (Hecobian et al.,
234 2010;Huang et al., 2018). On average, $Abs_{365,WS\text{-}BrC}$ is significantly higher than $Abs_{365,WI\text{-}BrC}$ in
235 summer (5.00±1.28 Mm^{-1} vs. 2.95±1.94 Mm^{-1}), but the values vary slightly in winter (19.6±8.3
236 Mm^{-1} vs. 21.9±13.5 Mm^{-1}). The substantially higher BrC absorptions in winter correspond to a
237 much higher organic aerosol concentration – WSOC and WIOC concentrations in winter are on
238 average 4.2 and 14 times of the concentrations in summer (Table 1). Elevated OA (organic
239 aerosols) concentration during winter is due to a combination of lower PBL height and enhanced
240 primary emissions (e.g., from residential heating) in the cold season. It is worth noting that the
241 wavelength-dependent Abs of WS-BrC shows a minor tip at about 360 nm in both seasons
242 (Figure 2), which may be related to the contribution of some specific chromophores. For
243 example, Lin et al. (2015) reported that some nitrogen-containing organic compounds (such as
244 picric acid or nitrophenol) have a maximum absorption at wavelength of ~360 nm. The tip
245 possibly caused an overestimation of average Abs and MAC at wavelength of 365 nm in this
246 study. However, the influence seems insignificant based on a comparison of average Abs and
247 MAC at wavelength of 340 nm, 350 nm, 360 nm, 370 nm, and 380 nm (Table S1).
248 The MACs of WS-BrC are comparable between the two seasons (Figure 2c & d), with the
249 average $MAC_{365,WS\text{-}BrC}$ being 1.00 (±0.18) $m^2\ g^{-1}$ in summer and 0.93 (±0.25) $m^2\ g^{-1}$ in winter
250 (Table 1). As summarized in Table 2, the $MAC_{365,WS\text{-}BrC}$ measured in this study, i.e., at a rural
251 site in the Guanzhong Basin of China, is comparable to or lower than the values observed in
252 Asian cities such Xi'an (Huang et al., 2018), Beijing (Cheng et al., 2011), Seoul (Kim et al.,

253 2016) and New Delhi (Kirillova et al., 2014b), but obviously higher than those in the regional
254 sites of North China Plain (Teich et al., 2017) and the background site of Tibetan Plateau (Xu et
255 al., 2020). Moreover, significantly lower $MAC_{365,WS\text{-}BrC}$ values were observed in the US,
256 including Los Angeles Basin (Zhang et al., 2013), Southeastern US (Hecobian et al., 2010), and
257 Atlanta (Liu et al., 2013).

258 In winter, the average $MAC_{365,WI\text{-}BrC}$ (0.95±0.32 m^2 g^{-1}) is comparable to $MAC_{365,WS\text{-}BrC}$
259 (0.93±0.25 m^2 g^{-1}; Table 1). However, in summer the $MAC_{365,WI\text{-}BrC}$ is much higher than
260 $MAC_{365,WS\text{-}BrC}$ (1.82±1.06 vs. 1.00±0.18 m^2 g^{-1}), indicating a relatively stronger light absorption
261 capability of hydrophobic chromophores than hydrophilic chromophores. Further, the fact that
262 the summertime $MAC_{365,WI\text{-}BrC}$ is nearly double the wintertime $MAC_{365,WI\text{-}BrC}$ suggests that more
263 light absorbing molecules are formed in the warm season.

264 Figure 2 compares the wavelength-dependent light absorptivity (i.e., Abs_λ and MAC_λ) of
265 WS-BrC and WI-BrC between day and night in summer and winter. Higher $Abs_{\lambda,WS\text{-}BrC}$ and
266 $Abs_{\lambda,WI\text{-}BrC}$ occurred during daytime in summer but during nighttime in winter. The MAC_λ of
267 WS-BrC are overall similar between daytime and nighttime in both seasons. However, the MAC_λ
268 of WI-BrC show a significant daytime increase in summer over the whole wavelength range of
269 300-700 nm (Figure 2c). The day-night change of BrC light absorptivity can be viewed more
270 obviously in Figure 1e and 1f, where the temporal variations of the Abs_{365} and MAC_{365} of WS-
271 BrC and WI-BrC during summer 2016 (Aug. 3-23) and winter 2017 (Jan. 20 -Feb. 1) are
272 presented. The highest day/night ratio of $MAC_{365,WIOC}$ reached 3.8 in summer and the average
273 daytime $MAC_{365,WI\text{-}BrC}$ in summer (2.45±1.14 m^2 g^{-1}) is more than twice the value during
274 nighttime (1.18±0.36 m^2 g^{-1}; Table 1). A possible reason for this observation is that there are

additional sources of WI-BrC during summer daytime in this rural region, such as secondary formation of hydrophobic light absorbing compounds.

Figure 3 and 4 present the cross-correlations of $Abs_{365,WS\text{-}BrC}$ and $Abs_{365,WI\text{-}BrC}$ with major chemical components (e.g., WSOC, WSIC, and sulfate) and molecular tracer species in summer and winter, respectively. In winter, $Abs_{365,WS\text{-}BrC}$ correlates strongly with WSOC concentration (r^2=0.80), so does $Abs_{365,WI\text{-}BrC}$ with WIOC (r^2=0.76). However, their relationships in summer are much weaker, especially for the correlation between $Abs_{365,WI\text{-}BrC}$ and WIOC (r^2=0.50). Considering that secondary OA (SOA) are mainly comprised of water-soluble compounds, such as polyalcohols/polyacids and phenols (Kondo et al., 2007), the much higher WSOC/OC ratio in summer (0.75±0.07) compared to winter (0.50±0.09) confirms more prevalent SOA formation in summer associated with higher temperature and stronger solar radiation. Formation of secondary organic chromophores may lead to a more complex composition of BrC in summer. More evidences on secondary BrC formation are provided in the subsequent sections.

Numerous studies reported that biomass burning is a dominant source of BrC in the atmosphere (Desyaterik et al., 2013;Washenfelder et al., 2015). In the current study, levoglucosan – a key tracer for biomass burning emissions (Simoneit, 2002) –was determined. As shown in Figure 3 and 4, levoglucosan correlates well with WSOC and WIOC in both summer and winter (r^2=0.45-0.77), suggesting that biomass burning is an important source of OA in the rural region of Guanzhong Basin. For most of the periods in this study, the $MAC_{365,WS\text{-}BrC}$ and $MAC_{365,WI\text{-}BrC}$ values are within the range of MAC of biomass burning aerosols (e.g., 1.3−1.8 for corn stalk (Li et al., 2016a), ~1.37 for rice straw (Park and Yu, 2016), ~1.9 for BB smoke particles (Lin et al., 2017)). Also, $Abs_{365,WI\text{-}BrC}$ in both summer and winter correlate well

297 with levoglusocan (r^2=0.74 and 0.62, respectively), demonstrating an important contribution of
298 biomass burning to WI-BrC despite the fact that levoglucosan itself is water soluble. The
299 relationships between the $Abs_{365,WS\text{-}BrC}$ and levoglucosan are much weaker (r^2=0.40 and 0.45 in
300 summer and winter, respectively), suggesting more complex sources of WS-BrC in the region.

301 **3.2 Molecular characterization of BrC aerosols**

302 Five categories of molecular tracer compounds, i.e., parent-polycyclic aromatic
303 hydrocarbons (parent-PAHs), oxygenated-PAHs (OPAHs), nitrophenols, isoprene-derived
304 products (SOA_i), and α-/β-pinene-derived products (SOA_p), were determined by the GC-EIMS
305 technique to investigate the formation pathways of BrC in this study. Their average
306 concentrations as well as daytime and nighttime differences are summarized in Table 1, and the
307 temporal variation profiles of the sum concentrations of each category, together with
308 levoglucosan time series, are presented in Figure S3.

309 PAHs and their oxidized products are important BrC chromophores, since the large
310 conjugated polycyclic structures are strongly light-absorbing in the near-UV range (Samburova
311 et al., 2016;Huang et al., 2018). A total number of 14 parent PAHs and 5 OPAHs (Table S2)
312 were determined in this study. Parent-PAHs are unsubstituted PAHs mainly emitted directly
313 from incomplete combustions of coal, biofuel, gasoline or other materials whereas OPAHs can
314 be emitted directly from combustion sources or formed from photochemical oxidation of the
315 parent-PAHs. The time trends of parent-PAHs and OPAHs are highly similar in both seasons (r^2
316 = 0.90 and 0.98 in summer and winter, respectively, Figure 3 and 4), suggesting that they have
317 common combustion sources. In addition, both parent-PAHs and OPAHs presented good
318 correlations with levoglucosan, particularly in winter (r^2 = 0.69 and 0.73, respectively; Figure 4),

indicating that biomass burning is an important contributor to ambient particulate PAHs in the region. PAHs, as well as levoglucosan, are elevated during nighttime in winter, corresponding to enhanced biomass burning emissions from heating-related activities as well as reduced boundary layer height at night. In contrast, the average daytime concentrations of parent-PAHs (11.6±5.7 ng m^{-3}) and levoglucosan (142±89 ng m^{-3}) in summer are about 1.95 and 2.58 times, respectively, of the values at night (Table 1). The daytime enhancement of OPAHs concentrations in summer is even more pronounced with an average day/night ratio of ~4.6 and as high as 9.8 for individual OPAH species (e.g., 6H-henzo(cd)pyrene-6-one; Figure S4). Both parent-PAHs and OPAHs, which are hydrophobic thus mainly exist as WIOC, demonstrate a good linear relationship with $Abs_{365,WI\text{-}BrC}$ in both winter and summer (r^2 = 0.49-0.83, Figure 3 and 3). However, the good correlation between OPAHs and $Abs_{365,WI\text{-}BrC}$ in summer appears to be mainly driven by daytime production, as the correlation coefficient (r^2) is 0.72 for the daytime data but is <0.1 for the nighttime data (Figure S5a). These results suggest that photochemical formation of light-absorption compounds is an important source of BrC during summer in the Guanzhong Basin.

We estimated the potential contribution of parent-PAHs and OPAHs to the light absorption of WI-BrC using a method reported in Samburova et al. (2016). Details on the method are presented in the Supplementary Information (SI). Table S3 summarizes the solar-spectrum-weighed mass absorption coefficients for PAHs ($MAC_{PAH,av}$) used in the calculation. As shown in Figure 5, the contribution of parent-PAHs to solar-spectrum-weighed absorption coefficient of WI-BrC varies between 0.55% - 0.66% with slight diurnal or season variations (Table S3). However, the contribution of OPAHs clearly shows higher daytime values, especially in

summer. The average contribution of OPAHs to the solar-spectrum-weighed absorption coefficient of WI-BrC in summer is 0.51±0.28% during daytime and 0.34±0.19% during nighttime. These results indicate that more secondary water-insoluble aromatic chromophores were produced via photochemical oxidation during summertime in the rural region.

Nitrophenols were identified as one of the most important light-absorbing compounds in particles and cloud water influenced by BB emission in China (Desyaterik et al., 2013). These compounds can be either directly emitted from burning of biomass (Xie et al., 2019) or formed in the atmosphere through gas phase and aqueous phase reactions of aromatic precursors including benz[a]pyrene (Lu et al., 2011), naphthalene (Kitanovski et al., 2014), catechol and guaiacol (Ofner et al., 2011), and toluene (Liu et al., 2015) in the presence of NO_x. In this study, only a few nitrophenol compounds were detected in PM (Table S2) and their average (±1σ) concentration is 0.94 (±0.26) ng m^{-3} in summer and 72.6 (±63.7) ng m^{-3} in winter. The wintertime concentrations of nitrophenols measured in the current study are comparable to those detected in Shanghai (Li et al., 2016b), Mt. Tai in the Shandong province of China (Desyaterik et al., 2013), and Ljubljana of Slovenia (Kitanovski et al., 2012), but the summertime concentrations observed are more comparable to those detected in the Los Angeles Basin of the U.S. (Zhang et al., 2013). The substantially lower concentration of nitrophenols in summer may be related to rapid photodegradation in the atmosphere. Indeed, according to a laboratory study conducted by Zhao et al. (2015) the timescale for photo-bleaching of nitrophenols can be an hour or less. Furthermore, as shown in Figure S5b, during wintertime, when low temperature and weak solar irradiation suppress photodegradation process, nitrophenols concentration anti-correlates with O_3 mixing ratio in a nonlinear manner (r^2=0.60). On average, concentration of

363 nitrophenols in winter is 2.5 times higher during nighttime than during daytime whereas the
364 nighttime concentrations of levoglucosan and PAHs are only slightly higher than the daytime
365 concentrations (by 11% and 33%, respectively; Table 1). Levoglucosan and PAHs are less
366 photochemically reactive than nitrophenols. These results confirm that nitrophenols, and other
367 photoreactive BrC compounds, may undergo significant atmospheric degradation during
368 summertime.

369 Both summertime and wintertime $Abs_{365,WS\text{-}BrC}$ correlated well with the concentrations of
370 nitrophenols (r^2=0.51-0.72, Figure S5c & d), suggesting an important contribution of nitrated
371 aromatic compounds to light absorption of WS-BrC in the study area. Using the MAC of
372 individual nitrophenol reported in Zhang et al. (2013), we calculated that the contributions of
373 nitrophenols to aerosol light absorption are 6.5-27 times higher than their mass contributions to
374 WSOC and that the fractions are much higher in winter (2.44±1.78%) than in summer
375 (0.12±0.03%; Table S3). In addition, due to a significantly higher abundance of nitrophenols
376 during nighttime in winter, their fractional contribution to aerosol absorption is on average 2.5
377 times higher than during the day (3.47±2.03% vs. 1.41±0.29%).

378 On a global scale, biogenic VOCs, mostly consisting of isoprene and monoterpenes, are
379 nearly an order of magnitude more abundant than anthropogenic VOCs (Guenther et al., 2006),
380 and their secondary products are estimated to be a predominant contributor to global SOA
381 burden (Heald et al., 2008). Recent studies (Lin et al., 2014;Nakayama et al., 2015;Nakayama et
382 al., 2012) showed that a large amount of biogenic SOA compounds are light absorptive. Some
383 tracers of SOA formed from isoprene (SOA_i) and α-/β-pinene (SOA_p) oxidation were measured
384 in the summertime samples (Table S2), and their temporal variations are shown in Figure S3. No

biogenic SOA tracer species were detectable in the winter samples in this study. Similar results were obtained in our previous study in the Mt. Hua of the Guanzhong Basin (Li, 2011). These findings are consistent with low emissions of biogenic VOCs and low oxidation rates in this region during cold seasons. The average concentrations of SOA_i and SOA_p tracers in summer are 18.6±9.7 and 22.0±6.7 ng m^{-3}, respectively. Neither SOA_i tracers nor SOA_p tracers showed significant correlations with the absorption coefficient of WSOC or WSIC, suggesting a low contribution of biogenic SOA to aerosol light absorption in the region. In addition, compared to the MAC values observed in this study, the MACs of biogenic SOA reported in literature are much lower, on average, by nearly an order of magnitude (Laskin et al., 2015), which further support an insignificant contribution of biogenic sources to BrC in this region. This finding is consistent with the fact that the Guanzhong Basin is a highly polluted region, where the major emission sources of organic aerosols are anthropogenic.

3.3 Variation of BrC during extreme haze events in winter

In recent years, extremely severe haze events with very high $PM_{2.5}$ concentrations (up to 500-600 μg m^{-3}) and low visibility (lower than 1 km) occurred frequently during wintertime in China (Huang et al., 2014). In this study, a heavy haze event occurred during Jan. 21-26 when $PM_{2.5}$ concentration at the rural site increased continuously from ~100 μg m^{-3} to 430 μg m^{-3} and visibility decreased from >10 km to ~1.4 km (Figure 1b & d). Similar to most haze events occurred in Northeast China, this event was associated with stagnant meteorological condition with low wind speed (<1 km s^{-1}), which promotes the accumulation of pollutants. In addition, secondary inorganic aerosol species, e.g., SO_4^{2-}, NO_3^- and NH_4^+, increased sharply (Figure 1d), which indicates secondary aerosol formation was enhanced during the haze event despite the low

solar irradiance and low O_3 concertation (e.g., 2 ~ 40 μg m^{-3}; Figure 1c) conditions. Recent studies by Wang et al. (2016) and Cheng et al. (2016) reported dramatic increases of secondary inorganic components, mainly sulfate, nitrate and ammonium (SNA), during haze periods in China and attributed the increases to enhanced aqueous reactions under high relative humidity (RH) conditions with NO_2 being an important oxidant. Moreover, Huang et al. (2014) observed that SOA also increased obviously during haze periods in winter. Indeed, as shown in Figure 4, SO_4^{2-} correlates well with RH (r^2=0.64) and NO_2 (r^2=0.56) in winter. In addition, $Abs_{365,WS\text{-}BrC,}$ which increases continuously during the haze period with a peak value at 43.3 Mm^{-1} (Figure 1e), correlates well with RH (r^2=0.65), sulfate (r^2=0.84) and NO_2 (r^2=0.70) (Figure 4). In contrast, $Abs_{365,WI\text{-}BrC}$ presents obvious diurnal variation during the haze period, and the correlation of RH (r^2=0.40), sulfate (r^2=0.46) and NO_2 (r^2=0.41) with $Abs_{365,WI\text{-}BrC}$ are also much weaker than those with $Abs_{365,WS\text{-}BrC}$. These results suggest that aqueous oxidation has played a role in the formation of WS-BrC (Laskin et al., 2015) during the haze period, although the stagnant meteorological condition with low wind speed can also promote its accumulation. This finding is consistent with our previous study conducted in Xi'an (Wu et al., 2020), which also found a secondary formation of BrC in winter by using stable carbon isotope composition analysis. In contrast, a slowly decreasing trend of $MAC_{365,WIOC}$ was observed during the haze period, suggesting that some of the water-insoluble BrC species were oxidized to form water-soluble chromophores, possibly through aqueous-phase reactions.

It is worthwhile to mention that Jan. 27, 2017 was the Chinese New Year's Eve and a large amount of fireworks were set off for celebration. During this night, the concentrations of $PM_{2.5}$, OC, EC, WSOC and WIOC as well as SNA were 25%-51% lower than their wintertime average

concentrations due to the higher wind speed favoring for atmospheric dispersion (Figure 1). However, the $MAC_{365,WS\text{-}BrC}$ (1.81) increased to about 2 times of its average value in winter, and $Abs_{365,WS\text{-}BrC}$ (20.5 Mm^{-1}) also showed a slight increase. Meanwhile, metal ions, which are abundant in fireworks (Wu et al., 2018;Jiang et al., 2015), such as K^+, Mg^{2+}, and Ca^{2+}increased substantially during the night as well (Figure S6). These results indicate that the increase of $MAC_{365,WSOC}$ during the Chinese New Year's Eve is likely mainly contributed by metal-containing light-absorbing compounds emitted from fireworks (Laskin et al., 2015;Tran et al., 2017).

3.4 Estimation of direct absorption of solar radiation by BrC

Since the light absorption of BrC is mainly in the UV spectral region, an important concern is that BrC can reduce the solar actinic flux and thus affect atmospheric photochemistry and tropospheric ozone production (Jacobson, 1998;Mohr et al., 2013). In this study, the direct absorptions of solar radiation by both WS-BrC and WI-BrC were estimated by using Eq 7. Figure S7 presents the incident solar irradiance and actinic flux spectra determined for the region under midday summer (Aug. 10, 2016 13:00 pm Beijing (BJ) time) and winter (Jan. 25, 2017 13:00 pm BJ time) conditions. Note that the local time at Guanzhong is ~ 1 hour later than the BJ time.

Table 3 presents a summary of the calculated direct solar absorptions of BrC. In summer, the direct attenuation of actinic flux by WS-BrC and WI-BrC are estimated at $1.55\times10^{14}\pm0.43\times10^{14}$ and $1.03\times10^{14}\pm0.64\times10^{14}$ quanta s^{-1} cm^{-2}, respectively, in the UV range (300-400 nm), which account for 0.83±0.23% and 0.53±0.33%, respectively, of the total down-welling radiation. In winter, the direct absorptions by BrC are higher with WS-BrC and WI-BrC

on average accounting for 1.67±0.72% and 2.07±1.24%, respectively, of the total down-welling radiation in the UV range. These results suggest that BrC may have a significant influence on atmospheric photochemistry in the UV range. In the visible spectral region (400 - 700 nm), the contributions of WS-BrC and WI-BrC to the total down-welling radiation are negligible – 0.10±0.03% and 0.07±0.05% in summer, and 0.15±0.06% and 0.15±0.08% in winter, respectively.

Another concern of BrC is that they can absorb solar irradiance to influence tropospheric temperature in a similar way as black carbon (BC) or elemental carbon (EC) (Feng et al., 2013;Laskin et al., 2015). In our study, the direct absorption of solar irradiance by WS-BrC and WI-BrC are estimated at 0.51±0.14 and 0.34±0.21 W m^{-2} in summer, and 0.57±0.25 and 0.68±0.41 W m^{-2} in winter in the UV range. To evaluate the contribution of BrC to total aerosol absorption, we also estimated the direct absorption of EC based on the Carbon Analyzer data according to the method described by Kirillova et al. (2014b) and Kirchstetter and Thatcher (2012) (see SI). The estimated contributions of light absorption of BrC relative to EC are shown in Table 3. In the visible region, the contribution is estimated at 10.0±3.52% in summer and 4.99±1.23% in winter for WS-BrC, and 6.19±2.42% and 4.51±1.44%, respectively, for WI-BrC. However, in the UV range, the fractions increase to 49.3±14.5% in summer and 25.9±5.47% in winter for WS-BrC, 29.4±11.0% and 29.0±10.4% for WI-BrC, which are within the range of the values reported in other regions in China (Huang et al., 2018), India (Kirillova et al., 2014b), and Korea (Kirillova et al., 2014a). On the other hand, the direct light absorption of WI-BrC represents a substantive contribution to that of total BrC in this study, which is about 40% in summer and more than 50% in winter in both UV and visible range, emphasizing the important

473 role that WI-BrC likely plays in atmospheric chemistry and the Earth's climate system,
474 especially in China.

475 **4. Summary and Conclusion**

476 Both WS-BrC and WI-BrC showed elevated Abs in winter (4-7 times higher than those in
477 summer), corresponding to much higher concentrations of WSOC and WIOC due to a
478 combination of lower PBL height and enhanced primary emissions (e.g., from residential
479 heating) in the cold season. No significant differences were found for the daytime and nighttime
480 MACs of WS-BrC in summer, or for the MACs of WS-BrC and WI-BrC in winter. However, the
481 average daytime $MAC_{365,WI\text{-}BrC}$ was more than twice the nighttime value in summer. We found
482 that the average daytime concentrations of both parent-PAHs and levoglucosan in summer were
483 around 2 times of the values at night and the daytime OPAHs concentration was more than 4
484 times of the nighttime value. Moreover, OPAHs well correlated with $Abs_{365,WI\text{-}BrC}$ in summer
485 during daytime (r^2=0.72) but not during nighttime (r^2<0.1). These results demonstrated that
486 photochemical formation of BrC and enhanced BB emissions (e.g., from cooking) contributed to
487 the higher daytime MACs in summer. In winter, the Abs of WS-BrC correlated strongly with
488 relative humidity, sulfate, and NO_2, suggesting that aqueous-phase reactions played an important
489 role in the formation of secondary BrC. $Abs_{365,WS\text{-}BrC}$ correlated well with the concentrations of
490 nitrophenols in both seasons, suggesting an important contribution of nitrated aromatic
491 compounds to light absorption of WS-BrC. However, this contribution is much lower in summer
492 due to faster photodegradation reactions of these compounds. WS-BrC and WI-BrC were
493 estimated to account for 0.83±0.23% and 0.53±0.33%, respectively, of the total down-welling
494 solar radiation in the UV range in summer, and 1.67±0.72% and 2.07±1.24%, respectively, in

winter. The substantive contribution of WI-BrC to total BrC absorption (~40% in summer and >50% in winter) emphasize the important role that WI-BrC likely plays in atmospheric chemistry and the Earth's climate system.

Author Contributions

J.J. Li, Q. Zhang, G.H. Wang, K.F. Ho, and J.J. Cao designed the experiment. J.J. Li, G.H. Wang, and K.F. Ho arranged the sample collection. J. Li, L. Liu and C. Wu collected the samples. J.J. Li, J. Li, J.Y. Wang, W.Q. Jiang, and L.J. Li analyzed the samples. J.J. Li, Q. Zhang, and G.H. Wang performed the data interpretation. J.J. Li, Q. Zhang, and G.H. Wang wrote the paper.

Acknowledgements

This work was financially supported by the program from National Nature Science Foundation of China (No. 41773117, 91644102, 41977332, 91543116). Jianjun Li also acknowledged the support of the Youth Innovation Promotion Association CAS (No. 2020407). The authors gratefully acknowledge National Center for Atmospheric Research for the provision of the solar actinic flux and irradiance data (TUV Quick Calculator, http://cprm.acom.ucar.edu/Models/TUV/Interactive_TUV/) used in this publication.

References

Andreae, M. O., and Gelencser, A.: Black carbon or brown carbon? The nature of light-absorbing carbonaceous aerosols, Atmos. Chem. Phys., 6, 3131-3148, 10.5194/acp-6-3131-2006, 2006.

Chang, J. L., and Thompson, J. E.: Characterization of colored products formed during irradiation of aqueous solutions containing H2O2 and phenolic compounds, Atmos. Environ., 44, 541-551, 10.1016/j.atmosenv.2009.10.042, 2010.

Chen, Y., and Bond, T. C.: Light absorption by organic carbon from wood combustion, Atmos. Chem. Phys., 10, 1773-1787, 10.5194/acp-10-1773-2010, 2010.

Chen, Y., Ge, X., Chen, H., Xie, X., Chen, Y., Wang, J., Ye, Z., Bao, M., Zhang, Y., and Chen, M.: Seasonal light absorption properties of water-soluble brown carbon in atmospheric fine particles in Nanjing, China, Atmos. Environ., 187, 230-240, 10.1016/j.atmosenv.2018.06.002, 2018.

Cheng, Y., He, K. B., Zheng, M., Duan, F. K., Du, Z. Y., Ma, Y. L., Tan, J. H., Yang, F. M., Liu, J. M., Zhang, X. L.,

Weber, R. J., Bergin, M. H., and Russell, A. G.: Mass absorption efficiency of elemental carbon and water-soluble organic carbon in Beijing, China, Atmos. Chem. Phys., 11, 11497-11510, 10.5194/acp-11-11497-2011, 2011.

Cheng, Y., Zheng, G., Wei, C., Mu, Q., Zheng, B., Wang, Z., Gao, M., Zhang, Q., He, K., Carmichael, G., Pöschl, U., and Su, H.: Reactive nitrogen chemistry in aerosol water as a source of sulfate during haze events in China, Science Advances, 2, 10.1126/sciadv.1601530, 10.1126/sciadv.1601530, 2016.

De Haan, D. O., Tapavicza, E., Riva, M., Cui, T. Q., Surratt, J. D., Smith, A. C., Jordan, M. C., Nilakantan, S., Almodovar, M., Stewart, T. N., de Loera, A., De Haan, A. C., Cazaunau, M., Gratien, A., Pangui, E., and Doussin, J. F.: Nitrogen-Containing, Light-Absorbing Oligomers Produced in Aerosol Particles Exposed to Methylglyoxal, Photolysis, and Cloud Cycling, Environ. Sci. Technol., 52, 4061-4071, 10.1021/acs.est.7b06105, 2018.

Desyaterik, Y., Sun, Y., Shen, X., Lee, T., Wang, X., Wang, T., and Collett Jr., J. L.: Speciation of "brown" carbon in cloud water impacted by agricultural biomass burning in eastern China, J. Geophys. Res.-Atmos., 118, 7389-7399, doi:10.1002/jgrd.50561, 2013.

Du, Z., He, K., Cheng, Y., Duan, F., Ma, Y., Liu, J., Zhang, X., Zheng, M., and Weber, R.: A yearlong study of water-soluble organic carbon in Beijing II: Light absorption properties, Atmos. Environ., 89, 235-241, 10.1016/j.atmosenv.2014.02.022, 2014.

Feng, Y., Ramanathan, V., and Kotamarthi, V. R.: Brown carbon: a significant atmospheric absorber of solar radiation?, Atmos. Chem. Phys., 13, 8607-8621, 10.5194/acp-13-8607-2013, 2013.

Guenther, A., Karl, T., Harley, P., Wiedinmyer, C., Palmer, P. I., and Geron, C.: Estimates of global terrestrial isoprene emissions using MEGAN (Model of Emissions of Gases and Aerosols from Nature), Atmos. Chem. Phys., 6, 3181-3210, 2006.

Heald, C. L., Henze, D. K., Horowitz, L. W., Feddema, J., Lamarque, J. F., Guenther, A., Hess, P. G., Vitt, F., Seinfeld, J. H., Goldstein, A. H., and Fung, I.: Predicted change in global secondary organic aerosol concentrations in response to future climate, emissions, and land use change, J. Geophys. Res.-Atmos., 113, doi: 10.1029/2007jd009092, 10.1029/2007jd009092, 2008.

Hecobian, A., Zhang, X., Zheng, M., Frank, N., Edgerton, E. S., and Weber, R. J.: Water-Soluble Organic Aerosol material and the light-absorption characteristics of aqueous extracts measured over the Southeastern United States, Atmos. Chem. Phys., 10, 5965-5977, 10.5194/acp-10-5965-2010, 2010.

Huang, R.-J., Zhang, Y., Bozzetti, C., Ho, K.-F., Cao, J.-J., Han, Y., Daellenbach, K. R., Slowik, J. G., Platt, S. M., Canonaco, F., Zotter, P., Wolf, R., Pieber, S. M., Bruns, E. A., Crippa, M., Ciarelli, G., Piazzalunga, A., Schwikowski, M., Abbaszade, G., Schnelle-Kreis, J., Zimmermann, R., An, Z., Szidat, S., Baltensperger, U., El Haddad, I., and Prevot, A. S. H.: High secondary aerosol contribution to particulate pollution during haze events in China, Nature, 514, 218-222, 10.1038/nature13774, 2014.

Huang, R.-J., Yang, L., Cao, J., Chen, Y., Chen, Q., Li, Y., Duan, J., Zhu, C., Dai, W., Wang, K., Lin, C., Ni, H., Corbin, J. C., Wu, Y., Zhang, R., Tie, X., Hoffmann, T., O'Dowd, C., and Dusek, U.: Brown Carbon Aerosol in Urban Xi'an, Northwest China: The Composition and Light Absorption Properties, Environ. Sci. Technol., 52, 6825-6833, 10.1021/acs.est.8b02386, 2018.

Jacobson, M. Z.: Studying the effects of aerosols on vertical photolysis rate coefficient and temperature profiles over an urban airshed, J. Geophys. Res.-Atmos., 103, 10593-10604, 10.1029/98jd00287, 1998.

Jiang, Q., Sun, Y. L., Wang, Z., and Yin, Y.: Aerosol composition and sources during the Chinese Spring Festival: fireworks, secondary aerosol, and holiday effects, Atmos. Chem. Phys., 15, 6023-6034, 10.5194/acp-15-6023-2015, 2015.

Kim, H., Kim, J. Y., Jin, H. C., Lee, J. Y., and Lee, S. P.: Seasonal variations in the light-absorbing properties of

572 water-soluble and insoluble organic aerosols in Seoul, Korea, Atmos. Environ., 129, 234-242,
573 https://doi.org/10.1016/j.atmosenv.2016.01.042, 2016.
574 Kirchstetter, T. W., Novakov, T., and Hobbs, P. V.: Evidence that the spectral dependence of light absorption by
575 aerosols is affected by organic carbon, J. Geophys. Res.-Atmos., 109, doi:10.1029/2004JD004999,
576 10.1029/2004jd004999, 2004.
577 Kirchstetter, T. W., and Thatcher, T. L.: Contribution of organic carbon to wood smoke particulate matter absorption
578 of solar radiation, Atmos. Chem. Phys., 12, 6067-6072, 10.5194/acp-12-6067-2012, 2012.
579 Kirillova, E. N., Andersson, A., Han, J., Lee, M., and Gustafsson, Ö.: Sources and light absorption of water-soluble
580 organic carbon aerosols in the outflow from northern China, Atmos. Chem. Phys., 14, 1413-1422, 10.5194/acp-
581 14-1413-2014, 2014a.
582 Kirillova, E. N., Andersson, A., Tiwari, S., Srivastava, A. K., Bisht, D. S., and Gustafsson, Ö.: Water-soluble organic
583 carbon aerosols during a full New Delhi winter: Isotope-based source apportionment and optical properties, J.
584 Geophys. Res.-Atmos., 119, 3476-3485, 10.1002/2013jd020041, 2014b.
585 Kirillova, E. N., Marinoni, A., Bonasoni, P., Vuillermoz, E., Facchini, M. C., Fuzzi, S., and Decesari, S.: Light
586 absorption properties of brown carbon in the high Himalayas, J. Geophys. Res.-Atmos., 121, 9621-9639,
587 10.1002/2016jd025030, 2016.
588 Kitanovski, Z., Grgić, I., Vermeylen, R., Claeys, M., and Maenhaut, W.: Liquid chromatography tandem mass
589 spectrometry method for characterization of monoaromatic nitro-compounds in atmospheric particulate matter,
590 Journal of Chromatography A, 1268, 35-43, https://doi.org/10.1016/j.chroma.2012.10.021, 2012.
591 Kitanovski, Z., Čusak, A., Grgić, I., and Claeys, M.: Chemical characterization of the main products formed through
592 aqueous-phase photonitration of guaiacol, Atmos. Meas. Tech., 7, 2457-2470, 10.5194/amt-7-2457-2014, 2014.
593 Kondo, Y., Miyazaki, Y., Takegawa, N., Miyakawa, T., Weber, R. J., Jimenez, J. L., Zhang, Q., and Worsnop, D. R.:
594 Oxygenated and water-soluble organic aerosols in Tokyo, Journal of Geophysical Research, 112, doi:
595 10.1029/2006jd007056, 10.1029/2006jd007056, 2007.
596 Laskin, A., Laskin, J., and Nizkorodov, S. A.: Chemistry of Atmospheric Brown Carbon, Chemical reviews, 4335-
597 4382, 10.1021/cr5006167, 2015.
598 Laskin, J., Laskin, A., Roach, P. J., Slysz, G. W., Anderson, G. A., Nizkorodov, S. A., Bones, D. L., and Nguyen, L.
599 Q.: High-Resolution Desorption Electrospray Ionization Mass Spectrometry for Chemical Characterization of
600 Organic Aerosols, Analytical Chemistry, 82, 2048-2058, 10.1021/ac902801f, 2010.
601 Lee, H. J., Aiona, P. K., Laskin, A., Laskin, J., and Nizkorodov, S. A.: Effect of Solar Radiation on the Optical
602 Properties and Molecular Composition of Laboratory Proxies of Atmospheric Brown Carbon, Environ. Sci.
603 Technol., 48, 10217-10226, 10.1021/es502515r, 2014.
604 Li, J., Wang, G., Aggarwal, S. G., Huang, Y., Ren, Y., Zhou, B., Singh, K., Gupta, P. K., Cao, J., and Zhang, R.:
605 Comparison of abundances, compositions and sources of elements, inorganic ions and organic compounds in
606 atmospheric aerosols from Xi'an and New Delhi, two megacities in China and India, Science of The Total
607 Environment, 476–477, 485-495, http://dx.doi.org/10.1016/j.scitotenv.2014.01.011, 2014.
608 Li, J. J.: Chemical Composition, Size distribution and Source Apportionment of Atmospheric Aerosols at an Alpine
609 Site in Guanzhong Plain, China (in Chinese), Ph. D, Xi'an Jiaotong University, Xi'an, 124 pp., 2011.
610 Li, X., Chen, Y., and Bond, T. C.: Light absorption of organic aerosol from pyrolysis of corn stalk, Atmos. Environ.,
611 144, 249-256, https://doi.org/10.1016/j.atmosenv.2016.09.006, 2016a.
612 Li, X., Jiang, L., Hoa, L. P., Lyu, Y., Xu, T. T., Yang, X., Iinuma, Y., Chen, J. M., and Herrmann, H.: Size distribution
613 of particle-phase sugar and nitrophenol tracers during severe urban haze episodes in Shanghai, Atmos.
614 Environ., 145, 115-127, 10.1016/j.atmosenv.2016.09.030, 2016b.
615 Lin, P., Liu, J., Shilling, J. E., Kathmann, S. M., Laskin, J., and Laskin, A.: Molecular characterization of brown

carbon (BrC) chromophores in secondary organic aerosol generated from photo-oxidation of toluene, Phys Chem Chem Phys, 17, 23312-23325, 10.1039/c5cp02563j, 2015.
Lin, P., Bluvshtein, N., Rudich, Y., Nizkorodov, S. A., Laskin, J., and Laskin, A.: Molecular Chemistry of Atmospheric Brown Carbon Inferred from a Nationwide Biomass Burning Event, Environ Sci Technol, 51, 11561-11570, 10.1021/acs.est.7b02276, 2017.
Lin, Y.-H., Budisulistiorini, S. H., Chu, K., Siejack, R. A., Zhang, H., Riva, M., Zhang, Z., Gold, A., Kautzman, K. E., and Surratt, J. D.: Light-Absorbing Oligomer Formation in Secondary Organic Aerosol from Reactive Uptake of Isoprene Epoxydiols, Environ. Sci. Technol., 48, 12012-12021, 10.1021/es503142b, 2014.
Liu, J., Bergin, M., Guo, H., King, L., Kotra, N., Edgerton, E., and Weber, R. J.: Size-resolved measurements of brown carbon in water and methanol extracts and estimates of their contribution to ambient fine-particle light absorption, Atmos. Chem. Phys., 13, 12389-12404, 10.5194/acp-13-12389-2013, 2013.
Liu, J., Lin, P., Laskin, A., Laskin, J., Kathmann, S. M., Wise, M., Caylor, R., Imholt, F., Selimovic, V., and Shilling, J. E.: Optical properties and aging of light-absorbing secondary organic aerosol, Atmos. Chem. Phys., 16, 12815-12827, 10.5194/acp-16-12815-2016, 2016.
Liu, J., Mo, Y., Ding, P., Li, J., Shen, C., and Zhang, G.: Dual carbon isotopes (C-14 and C-13) and optical properties of WSOC and HULIS-C during winter in Guangzhou, China, Science of the Total Environment, 633, 1571-1578, 10.1016/j.scitotenv.2018.03.293, 2018.
Liu, P. F., Abdelmalki, N., Hung, H. M., Wang, Y., Brune, W. H., and Martin, S. T.: Ultraviolet and visible complex refractive indices of secondary organic material produced by photooxidation of the aromatic compounds toluene and m-xylene, Atmos. Chem. Phys., 15, 1435-1446, 10.5194/acp-15-1435-2015, 2015.
Lu, J. W., Flores, J. M., Lavi, A., Abo-Riziq, A., and Rudich, Y.: Changes in the optical properties of benzo[a]pyrene-coated aerosols upon heterogeneous reactions with NO2 and NO3, Physical Chemistry Chemical Physics, 13, 6484-6492, 10.1039/C0CP02114H, 2011.
Mohr, C., Lopez-Hilfiker, F. D., Zotter, P., Prévôt, A. S. H., Xu, L., Ng, N. L., Herndon, S. C., Williams, L. R., Franklin, J. P., Zahniser, M. S., Worsnop, D. R., Knighton, W. B., Aiken, A. C., Gorkowski, K. J., Dubey, M. K., Allan, J. D., and Thornton, J. A.: Contribution of Nitrated Phenols to Wood Burning Brown Carbon Light Absorption in Detling, United Kingdom during Winter Time, Environ. Sci. Technol., 47, 6316-6324, 10.1021/es400683v, 2013.
Moschos, V., Kumar, N. K., Daellenbach, K. R., Baltensperger, U., Prévôt, A. S. H., and El Haddad, I.: Source Apportionment of Brown Carbon Absorption by Coupling Ultraviolet–Visible Spectroscopy with Aerosol Mass Spectrometry, Environmental Science & Technology Letters, 5, 302-308, 10.1021/acs.estlett.8b00118, 2018.
Nakayama, T., Sato, K., Matsumi, Y., Imamura, T., Yamazaki, A., and Uchiyama, A.: Wavelength Dependence of Refractive Index of Secondary Organic Aerosols Generated during the Ozonolysis and Photooxidation of α-Pinene, SOLA, 8, 119-123, 10.2151/sola.2012-030, 2012.
Nakayama, T., Sato, K., Tsuge, M., Imamura, T., and Matsumi, Y.: Complex refractive index of secondary organic aerosol generated from isoprene/NOx photooxidation in the presence and absence of SO2, J. Geophys. Res.-Atmos., 120, 7777-7787, 10.1002/2015jd023522, 2015.
Nguyen, T. B., Lee, P. B., Updyke, K. M., Bones, D. L., Laskin, J., Laskin, A., and Nizkorodov, S. A.: Formation of nitrogen- and sulfur-containing light-absorbing compounds accelerated by evaporation of water from secondary organic aerosols, J. Geophys. Res.-Atmos., 117, 14, 10.1029/2011jd016944, 2012.
Nozière, B., and Esteve, W.: Organic reactions increasing the absorption index of atmospheric sulfuric acid aerosols, Geophysical Research Letters, 32, doi:10.1029/2004GL021942, 10.1029/2004gl021942, 2005.
Nozière, B., Dziedzic, P., and Córdova, A.: Formation of secondary light-absorbing “fulvic-like” oligomers: A common process in aqueous and ionic atmospheric particles?, Geophysical Research Letters, 34,

doi:10.1029/2007GL031300, 10.1029/2007gl031300, 2007.
Ofner, J., Krüger, H. U., Grothe, H., Schmitt-Kopplin, P., Whitmore, K., and Zetzsch, C.: Physico-chemical characterization of SOA derived from catechol and guaiacol – a model substance for the aromatic fraction of atmospheric HULIS, Atmos. Chem. Phys., 11, 1-15, 10.5194/acp-11-1-2011, 2011.
Park, S. S., and Yu, J.: Chemical and light absorption properties of humic-like substances from biomass burning emissions under controlled combustion experiments, Atmos. Environ., 136, 114-122, https://doi.org/10.1016/j.atmosenv.2016.04.022, 2016.
Powelson, M. H., Espelien, B. M., Hawkins, L. N., Galloway, M. M., and De Haan, D. O.: Brown Carbon Formation by Aqueous-Phase Carbonyl Compound Reactions with Amines and Ammonium Sulfate, Environ. Sci. Technol., 48, 985-993, 10.1021/es4038325, 2014.
Rizzo, L. V., Correia, A. L., Artaxo, P., Procópio, A. S., and Andreae, M. O.: Spectral dependence of aerosol light absorption over the Amazon Basin, Atmos. Chem. Phys., 11, 8899-8912, 10.5194/acp-11-8899-2011, 2011.
Rizzo, L. V., Artaxo, P., Müller, T., Wiedensohler, A., Paixão, M., Cirino, G. G., Arana, A., Swietlicki, E., Roldin, P., Fors, E. O., Wiedemann, K. T., Leal, L. S. M., and Kulmala, M.: Long term measurements of aerosol optical properties at a primary forest site in Amazonia, Atmos. Chem. Phys., 13, 2391-2413, 10.5194/acp-13-2391-2013, 2013.
Romonosky, D. E., Laskin, A., Laskin, J., and Nizkorodov, S. A.: High-Resolution Mass Spectrometry and Molecular Characterization of Aqueous Photochemistry Products of Common Types of Secondary Organic Aerosols, The Journal of Physical Chemistry A, 119, 2594-2606, 10.1021/jp509476r, 2015.
Samburova, V., Connolly, J., Gyawali, M., Yatavelli, R. L. N., Watts, A. C., Chakrabarty, R. K., Zielinska, B., Moosmüller, H., and Khlystov, A.: Polycyclic aromatic hydrocarbons in biomass-burning emissions and their contribution to light absorption and aerosol toxicity, Science of The Total Environment, 568, 391-401, https://doi.org/10.1016/j.scitotenv.2016.06.026, 2016.
Sengupta, D., Samburova, V., Bhattarai, C., Kirillova, E., Mazzoleni, L., Iaukea-Lum, M., Watts, A., Moosmuller, H., and Khlystov, A.: Light absorption by polar and non-polar aerosol compounds from laboratory biomass combustion, Atmos. Chem. Phys., 18, 10849-10867, 10.5194/acp-18-10849-2018, 2018.
Shen, Z., Zhang, Q., Cao, J., Zhang, L., Lei, Y., Huang, Y., Huang, R. J., Gao, J., Zhao, Z., Zhu, C., Yin, X., Zheng, C., Xu, H., and Liu, S.: Optical properties and possible sources of brown carbon in PM 2.5 over Xi'an, China, Atmos. Environ., 150, 322-330, 10.1016/j.atmosenv.2016.11.024, 2017.
Simoneit, B. R. T.: Biomass burning - A review of organic tracers for smoke from incomplete combustion, Applied Geochemistry, 17, 129-162, 2002.
Smith, J. D., Kinney, H., and Anastasio, C.: Phenolic carbonyls undergo rapid aqueous photodegradation to form low-volatility, light-absorbing products, Atmos. Environ., 126, 36-44, 10.1016/j.atmosenv.2015.11.035, 2016.
Sumlin, B. J., Pandey, A., Walker, M. J., Pattison, R. S., Williams, B. J., and Chakrabarty, R. K.: Atmospheric Photooxidation Diminishes Light Absorption by Primary Brown Carbon Aerosol from Biomass Burning, Environmental Science & Technology Letters, 4, 540-545, 10.1021/acs.estlett.7b00393, 2017.
Sun, H., Biedermann, L., and Bond, T. C.: Color of brown carbon: A model for ultraviolet and visible light absorption by organic carbon aerosol, Geophysical Research Letters, 34, doi: 10.1029/2007gl029797, 10.1029/2007gl029797, 2007.
Teich, M., van Pinxteren, D., Wang, M., Kecorius, S., Wang, Z., Müller, T., Močnik, G., and Herrmann, H.: Contributions of nitrated aromatic compounds to the light absorption of water-soluble and particulate brown carbon in different atmospheric environments in Germany and China, Atmos. Chem. Phys., 17, 1653-1672, 10.5194/acp-17-1653-2017, 2017.
Tran, A., Williams, G., Younus, S., Ali, N. N., Blair, S. L., Nizkorodov, S. A., and Al-Abadleh, H. A.: Efficient

Formation of Light-Absorbing Polymeric Nanoparticles from the Reaction of Soluble Fe(III) with C4 and C6 Dicarboxylic Acids, Environ. Sci. Technol., 51, 9700-9708, 10.1021/acs.est.7b01826, 2017.

Updyke, K. M., Nguyen, T. B., and Nizkorodov, S. A.: Formation of brown carbon via reactions of ammonia with secondary organic aerosols from biogenic and anthropogenic precursors, Atmos. Environ., 63, 22-31, https://doi.org/10.1016/j.atmosenv.2012.09.012, 2012.

van Donkelaar, A., Martin, R. V., Brauer, M., Kahn, R., Levy, R., Verduzco, C., and Villeneuve, P. J.: Global Estimates of Ambient Fine Particulate Matter Concentrations from Satellite-Based Aerosol Optical Depth: Development and Application, Environmental Health Perspectives, 118, 847-855, 10.1289/ehp.0901623, 2010.

Wang, G. H., Zhang, R. Y., Gomez, M. E., Yang, L. X., Zamora, M. L., Hu, M., Lin, Y., Peng, J. F., Guo, S., Meng, J. J., Li, J. J., Cheng, C. L., Hu, T. F., Ren, Y. Q., Wang, Y. S., Gao, J., Cao, J. J., An, Z. S., Zhou, W. J., Li, G. H., Wang, J. Y., Tian, P. F., Marrero-Ortiz, W., Secrest, J., Du, Z. F., Zheng, J., Shang, D. J., Zeng, L. M., Shao, M., Wang, W. G., Huang, Y., Wang, Y., Zhu, Y. J., Li, Y. X., Hu, J. X., Pan, B., Cai, L., Cheng, Y. T., Ji, Y. M., Zhang, F., Rosenfeld, D., Liss, P. S., Duce, R. A., Kolb, C. E., and Molina, M. J.: Persistent sulfate formation from London Fog to Chinese haze, Proceedings of the National Academy of Sciences of the United States of America, 113, 13630-13635, 10.1073/pnas.1616540113, 2016.

Washenfelder, R. A., Attwood, A. R., Brock, C. A., Guo, H., Xu, L., Weber, R. J., Ng, N. L., Allen, H. M., Ayres, B. R., Baumann, K., Cohen, R. C., Draper, D. C., Duffey, K. C., Edgerton, E., Fry, J. L., Hu, W. W., Jimenez, J. L., Palm, B. B., Romer, P., Stone, E. A., Wooldridge, P. J., and Brown, S. S.: Biomass burning dominates brown carbon absorption in the rural southeastern United States, Geophysical Research Letters, 42, 653-664, doi:10.1002/2014GL062444, 2015.

Wu, C.: Seasonal variation of atmospheric acidic and basic species and the characteristics of gas-particle partition in a typical city of Guanzhong Basin (in Chinese), Ph. D, The University of Chinese Academy of Sciences, The University of Chinese Academy of Sciences, Xi'an, 2018.

Wu, C., Wang, G., Wang, J., Li, J., Ren, Y., Zhang, L., Cao, C., Li, J., Ge, S., Xie, Y., Wang, X., and Xue, G.: Chemical characteristics of haze particles in Xi'an during Chinese Spring Festival: Impact of fireworks burning, Journal of Environmental Sciences, 71, 179-187, https://doi.org/10.1016/j.jes.2018.04.008, 2018.

Wu, C., Wang, G., Li, J., Li, J., Cao, C., Ge, S., Xie, Y., Chen, J., Li, X., Xue, G., Wang, X., Zhao, Z., and Cao, F.: The characteristics of atmospheric brown carbon in Xi'an, inland China: sources, size distributions and optical properties, Atmos. Chem. Phys., 20, 2017-2030, 10.5194/acp-20-2017-2020, 2020.

Wu, G., Ram, K., Fu, P., Wang, W., Zhang, Y., Liu, X., Stone, E. A., Pradhan, B. B., Dangol, P. M., Panday, A. K., Wan, X., Bai, Z., Kang, S., Zhang, Q., and Cong, Z.: Water-Soluble Brown Carbon in Atmospheric Aerosols from Godavari (Nepal), a Regional Representative of South Asia, Environ. Sci. Technol., 53, 3471-3479, 10.1021/acs.est.9b00596, 2019.

Xie, M., Chen, X., Hays, M. D., and Holder, A. L.: Composition and light absorption of N-containing aromatic compounds in organic aerosols from laboratory biomass burning, Atmos. Chem. Phys., 19, 2899-2915, 10.5194/acp-19-2899-2019, 2019.

Xu, J., Cui, T. Q., Fowler, B., Fankhauser, A., Yang, K., Surratt, J. D., and McNeill, V. F.: Aerosol Brown Carbon from Dark Reactions of Syringol in Aqueous Aerosol Mimics, Acs Earth and Space Chemistry, 2, 608-617, 10.1021/acsearthspacechem.8b00010, 2018.

Xu, J., Hettiyadura, A. P. S., Liu, Y., Zhang, X., Kang, S., and Laskin, A.: Regional Differences of Chemical Composition and Optical Properties of Aerosols in the Tibetan Plateau, Journal of Geophysical Research: Atmospheres, 125, 10.1029/2019jd031226, 2020.

Yan, C., Zheng, M., Sullivan, A. P., Bosch, C., Desyaterik, Y., Andersson, A., Li, X., Guo, X., Zhou, T., Gustafsson, Ö., and Collett, J. L.: Chemical characteristics and light-absorbing property of water-soluble organic carbon in

Beijing: Biomass burning contributions, Atmos. Environ., 121, 4-12, https://doi.org/10.1016/j.atmosenv.2015.05.005, 2015a.

Yan, C., Zheng, M., Sullivan, A. P., Bosch, C., Desyaterik, Y., Andersson, A., Li, X., Guo, X., Zhou, T., Gustafsson, O., and Collett, J. L., Jr.: Chemical characteristics and light-absorbing property of water-soluble organic carbon in Beijing: Biomass burning contributions, Atmos. Environ., 121, 4-12, 10.1016/j.atmosenv.2015.05.005, 2015b.

Yan, C. Q., Zheng, M., Bosch, C., Andersson, A., Desyaterik, Y., Sullivan, A. P., Collett, J. L., Zhao, B., Wang, S. X., He, K. B., and Gustafsson, O.: Important fossil source contribution to brown carbon in Beijing during winter, Scientific reports, 7, DOI: 10.1038/srep43182, 10.1038/srep43182, 2017.

Yu, L., Smith, J., Laskin, A., Anastasio, C., Laskin, J., and Zhang, Q.: Chemical characterization of SOA formed from aqueous-phase reactions of phenols with the triplet excited state of carbonyl and hydroxyl radical, Atmos. Chem. Phys., 14, 13801-13816, 10.5194/acp-14-13801-2014, 2014.

Zhang, X., Lin, Y.-H., Surratt, J. D., and Weber, R. J.: Sources, Composition and Absorption Ångström Exponent of Light-absorbing Organic Components in Aerosol Extracts from the Los Angeles Basin, Environ. Sci. Technol., 47, 3685-3693, 10.1021/es305047b, 2013.

Zhao, R., Lee, A. K. Y., Huang, L., Li, X., Yang, F., and Abbatt, J. P. D.: Photochemical processing of aqueous atmospheric brown carbon, Atmos. Chem. Phys., 15, 6087-6100, 10.5194/acp-15-6087-2015, 2015.

Table 1 Average (±1σ) values Abs_{365}, MAC_{365}, and AAE of WS-BrC and WI-BrC, as well as concentrations of OC, WSOC, WIOC, and measured organic species in the $PM_{2.5}$ aerosols from the rural site of Guanzhong Basin.

	Summer			Winter		
	Average	Daytime	Nighttime	Average	Daytime	Nighttime
$Abs_{365,WS\text{-}BrC}$ (Mm^{-1})	5.00±1.28	5.64±1.34	4.37±0.83	19.6±8.3	19.2±6.8	19.9±9.5
$Abs_{365,WI\text{-}BrC}$ (Mm^{-1})	2.95±1.94	4.23±1.93	1.67±0.72	21.9±13.5	17.2±8.2	26.7±15.8
$MAC_{365,WS\text{-}BrC}$ ($m^2\ g^{-1}$)	1.00±0.18	0.99±0.17	1.01±0.18	0.93±0.25	0.92±0.21	0.94±0.28
$MAC_{365,WI\text{-}BrC}$ ($m^2\ g^{-1}$)	1.82±1.06	2.45±1.14	1.18±0.36	0.95±0.32	0.85±0.34	1.05±0.28
$AAE_{WS\text{-}BrC}$	5.43±0.41	5.56±0.4	5.30±0.38	5.11±0.53	5.14±0.2	5.07±0.72
$AAE_{WI\text{-}BrC}$	5.01±0.58	4.74±0.19	5.28±0.71	6.04±0.22	5.94±0.12	6.15±0.24
OC (μg m^{-3})	6.78±1.77	7.74±1.73	5.83±1.19	45.9±22.9	44.0±17.2	47.9±27.2
WSOC (μg m^{-3})	5.06±1.11	5.72±1.02	4.39±0.72	21.9±9.3	22.1±8.0	21.7±10.4
WIOC (μg m^{-3})	1.73±0.87	2.02±1.04	1.44±0.53	24.0±14.3	21.9±10.1	26.2±17.3
WSOC/OC	0.75±0.07	0.75±0.09	0.76±0.04	0.50±0.09	0.51±0.08	0.48±0.10
Parent-PAHs (ng m^{-3})	8.81±5.09	11.6±5.7	5.98±1.9	82.3±53.7	70.8±35.4	93.9±65.1
OPAHs (ng m^{-3})	14.0±14.0	23.0±15.1	4.97±1.34	98.3±59.5	89.4±39.8	107±73
Nitrophenols (ng m^{-3})	0.94±0.26	0.87±0.26	1.02±0.24	72.6±63.7	41.1±15.5	104±77
SOA_i [a] (ng m^{-3})	18.6±9.7	15.0±8.0	22.1±9.8	BDL[c]	BDL	BDL
SOA_p [b] (ng m^{-3})	22.0±6.7	25.2±6.7	18.9±5.0	BDL	BDL	BDL
Levoglucosan (ng m^{-3})	98.7±83.7	142±89	55.1±48.7	601±301	569±138	633±401

[a] SOA_i: Tracers of SOA formed from isoprene (SOAi) oxidation, i.e., the sum of 2-methylglyceric acid, 2-methylthreitol, and 2-methylerythritol.

[b] SOA_i: Tracers of SOA formed from α-/β-pinene (SOAp) oxidation, i.e., the sum of pinonic acid, pinic acid, and 3-methyl-1,2,3-butanetricarboxylic acid.

[c] BDL: below detection limit (<0.17 ng m^{-3}) .

775 Table 2 Comparison of $MAC_{365,WS\text{-}BrC}$ in the present study and those reported in earlier studies in China, India, and
776 the United States (US).

Sampling site	Sampling time	Season	$MAC_{365,WS\text{-}BrC}$ (m^2 g^{-1})	Reference
Lincun, Shaanxi, China	Aug. 3-23, 2016	Summer	1.00±0.18	This study
	Jan. 20-Feb 1, 2017	Winter	0.93±0.25	
Xi'an, China	Jun. 1-Aug. 31, 2009	Summer	0.98 ±0.21	Huang et al. (2018)
	Nov.15, 2008-Mar. 14, 2009	Winter	1.65 ± 0.36	
Beijing, China	Jun. 20-Jul. 20, 2009	Summer	1.8 ± 0.2	Cheng et al. (2011)
	Jan.9-Feb. 12, 2009	Winter	0.7 ± 0.2	
XiangHe, Hebei, China	Jul. 9-14 and Jul. 21-Aug. 1, 2013	Summer	0.38 ± 0.52[a]	Teich et al. (2017)
Wangdu, Hebei, China	Jun. 4-24, 2014	Summer	0.55 ± 0.15[a]	
Mt. Waliguan, Qinghai, China	Jul. 1–31, 2017	Summer	0.48	Xu et al. (2020)
Seoul, Korea	Aug. 13-Sep. 9, 2013	Summer	0.28	Kim et al. (2016)
	Jan. 9-Feb 8, 2013	Winter	1.02	
New Delhi, India	Oct. 24, 2010-Mar. 25, 2011	Winter	1.6 ± 0.5	Kirillova et al. (2014b)
Los Angeles Basin, US	mid-May - mid-June, 2010	Summer	0.71	Zhang et al. (2013)
Southeastern US	2007	Annually	0.3–0.7	Hecobian et al. (2010)
Atlanta, US	May 17-Sep. 29, 2012	Summer and Fall	0.14-0.53	Liu et al. (2013)

777 [a] Data at XiangHe and Wangdu were the averaged MAC of WSOC at wavelength of 370 nm (i.e., $MAC_{370,WS\text{-}BrC}$)

778

779

780

781 Table 3 Average direct solar absorption of water-soluble and water-insoluble BrC during summer and winter

	WSOC		WIOC	
	Summer	Winter	Summer	Winter
Actinic flux ($\times 10^{14}$ quanta s^{-1} cm^{-2})				
300-400 nm	1.55±0.43	2.14±0.92	1.03±0.64	2.53±1.52
400-700 nm	1.77±0.6	2.67±1.04	1.24±0.8	2.58±1.48
Irradiance (W m^{-2})				
300-400 nm	0.51±0.14	0.57±0.25	0.34±0.21	0.68±0.41
400-700 nm	0.49±0.17	0.57±0.22	0.35±0.23	0.55±0.32
Relative to EC (%)				
300-400 nm	49.4±14.5	25.9±5.47	29.4±11.0	29.0±10.4
400-700 nm	10.0±3.52	4.99±1.23	6.19±2.42	4.51±1.44

782

783

Figure Caption

Figure 1 Temporal variation of meteorological parameters (a and b), concentrations of major chemical compositions, Abs_{365}, MAC_{365}, and AAE of water-soluble and water-insoluble BrC in $PM_{2.5}$ from the rural area of Northwest China.

Figure 2 Average spectra of absorption coefficient (Abs_{λ}) (a,b) and mass absorption coefficient (MAC_{λ}) (c,d) of water-soluble (WS-BrC) and water-insoluble (WI-BrC) BrC during daytime and nighttime of summer and winter. Absorption Ångström exponent (AAE) is calculated by a linear regression of log Abs_{λ} versus log λ in the wavelength range of 300−450 nm.

Figure 3 Cross correlations between $Abs_{365,WS\text{-}BrC}$, $Abs_{365,WI\text{-}BrC}$, selected chemical compositions, and RH in summer. The numbers at the upper right denote the linear correlation coefficients (r^2) of the corresponding scatter plots.

Figure 4 Cross correlations between $Abs_{365,WS\text{-}BrC}$, $Abs_{365,WI\text{-}BrC}$, selected chemical compositions, and RH in winter. The numbers at the upper right denote the linear correlation coefficients (r^2) of the corresponding scatter plots.

Figure 5 Average contribution of parent-PAHs and OPAHs to the bulk light absorption of WI-BrC (300−700 nm) during daytime and nighttime of summer and winter.

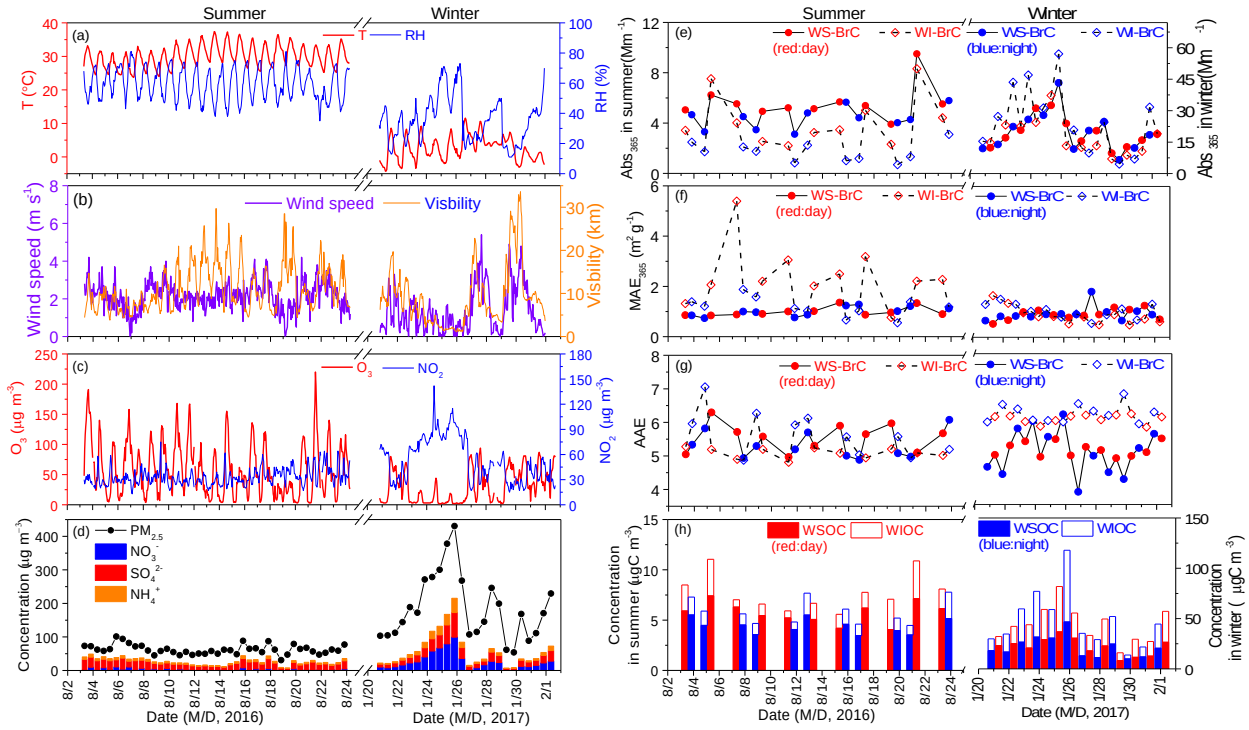

Figure 1 Temporal variation of meteorological parameters (a and b), concentrations of major chemical compositions, Abs_{365}, MAC_{365}, and AAE of water-soluble and water-insoluble BrC in $PM_{2.5}$ from the rural area of Northwest China.

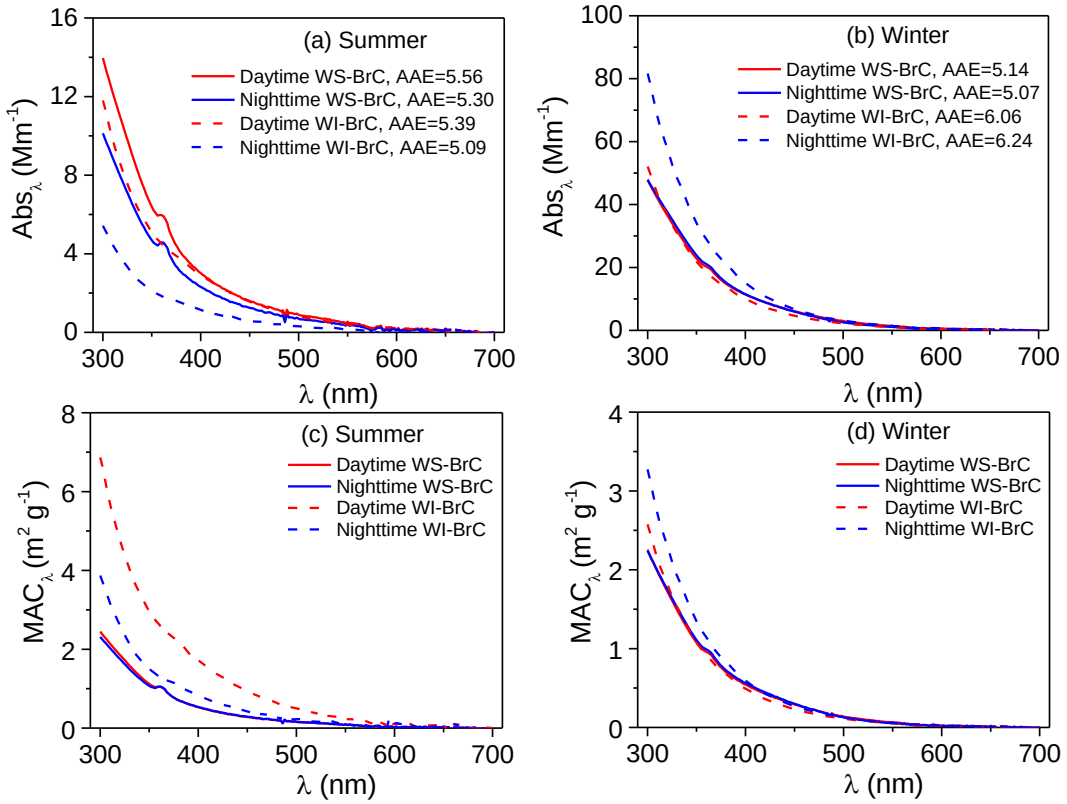

Figure 2 Average spectra of absorption coefficient (Abs$_\lambda$) (a,b) and mass absorption coefficient (MAC$_\lambda$) (c,d) of water-soluble (WS-BrC) and water-insoluble (WI-BrC) BrC during daytime and nighttime of summer and winter. Absorption Ångström exponent (AAE) is calculated by a linear regression of log Abs$_\lambda$ versus log λ in the wavelength range of 300−450 nm.

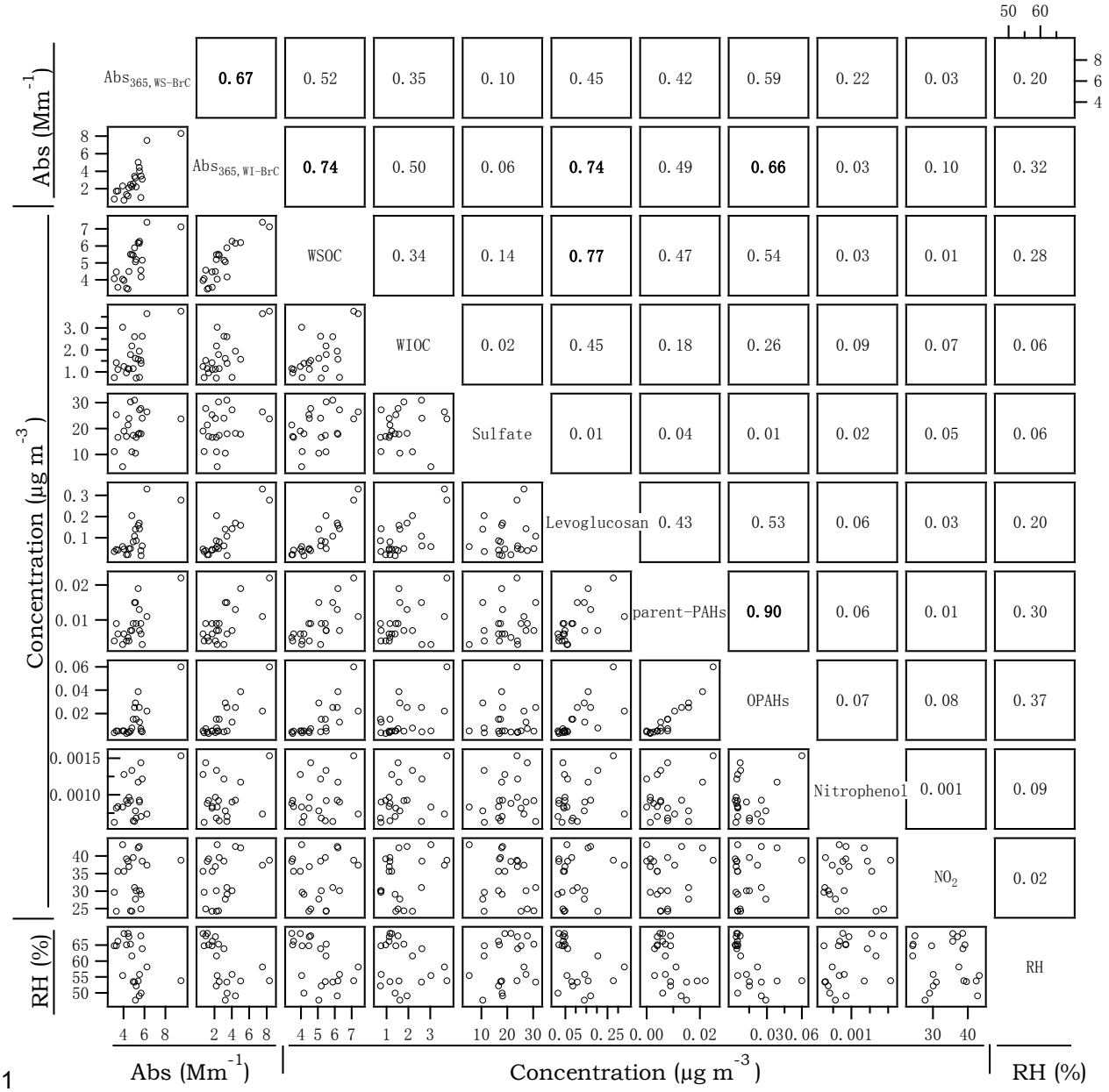

Figure 3 Cross-correlations between $Abs_{365,WS\text{-}BrC}$, $Abs_{365,WI\text{-}BrC}$, selected chemical components, and RH in summer. The numbers at the upper right denote the linear correlation coefficients (r^2) of the corresponding scatter plots.

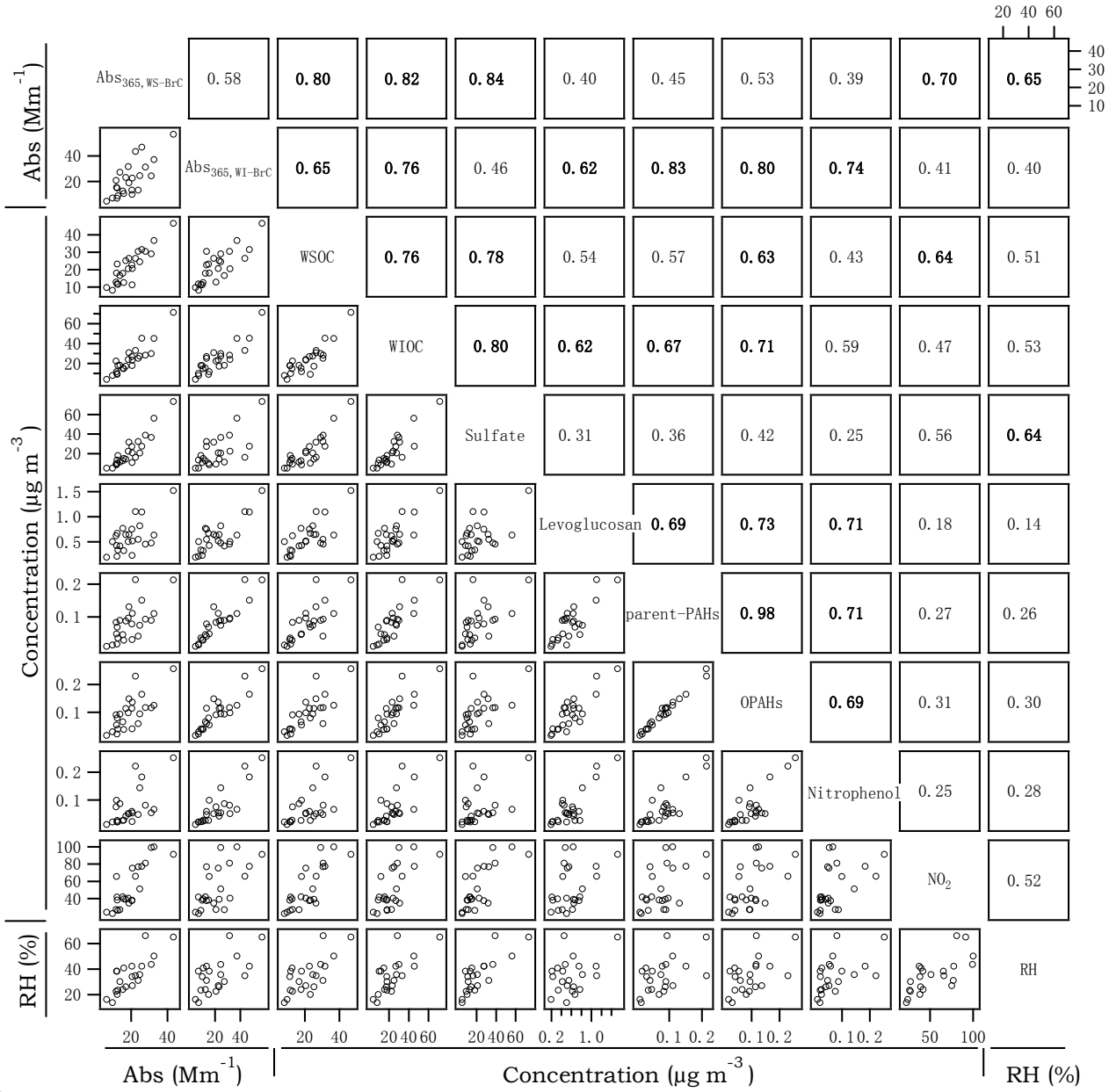

Figure 4 Cross-correlations between $Abs_{365,WS\text{-}BrC}$, $Abs_{365,WI\text{-}BrC}$, selected chemical components, and RH in winter. The numbers at the upper right denote the linear correlation coefficients (r^2) of the corresponding scatter plots.

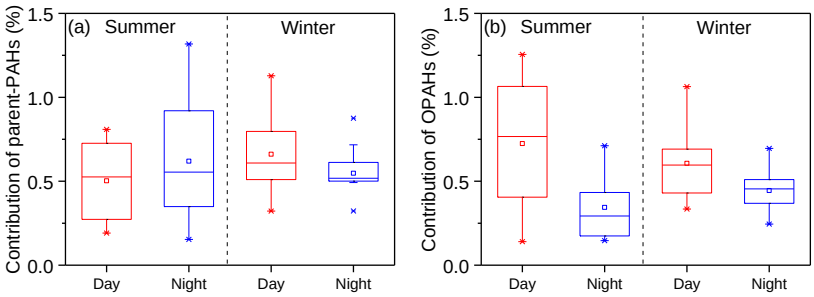

831

832 Figure 5 Average contribution of parent-PAHs and OPAHs to the bulk light absorption of WI-BrC (300−700
833 nm) during daytime and nighttime of summer and winter.

834

835